Available online at www.sciencedirect.com

SciVerse ScienceDirect

Advances in Space Research 49 (2012) 1598–1606

Advances in Space Research
(a COSPAR publication)

www.elsevier.com/locate/asr

What are the physical mechanisms of eruptions and CMEs?

Brigitte Schmieder *, Guillaume Aulanier

LESIA, Observatoire de Paris, CNRS, UPMC, Université Paris Diderot, 5 place Jules Janssen, 92190 Meudon, France

Received 15 July 2011; received in revised form 18 October 2011; accepted 19 October 2011
Available online 2 November 2011

Abstract

CMEs are due to physical phenomena that drive both, eruptions and flares in active regions. Eruptions/CMEs must be driven from initially force-free current-carrying magnetic field. Twisted flux ropes, sigmoids, current lanes and pattern in photospheric current maps show a clear evidence of currents parallel to the magnetic field. Eruptions occur starting from equilibria which have reached some instability threshold. Revisiting several data sets of CME observations we identified different mechanisms leading to this unstable state from a force free field. Boundary motions related to magnetic flux emergence and shearing favor the increase of coronal currents leading to the large flares of November 2003. On the other hand, we demonstrated by numerical simulations that magnetic flux emergence is not a sufficient condition for eruptions. Filament eruptions are interpreted either by a torus instability for an event occurring during the minimum of solar activity either by the diffusion of the magnetic flux reducing the tension of the restraining arcade. We concluded that CME models (tether cutting, break out, loss of equilibrium models) are based on these basic mechanisms for the onset of CMEs.

Keywords: Active region; Coronal mass ejection; MHD simulations of eruptions; Electric currents

1. Introduction

Coronal mass ejections (CMEs) are large volumes of magnetized plasma, which are ejected from the solar atmosphere into interplanetary space. They are formed by the eruption of low altitude coronal structures, predominantly located within active regions. Subramanian and Dere (2001) based on a sample of 32 CMEs found that 85% are associated with active regions and 15% of CMEs are related to so-called quiet regions. These are due to eruption of quiescent filaments not embedded in active regions (Schmieder, 2006). Therefore these CMEs are frequently related to large magnetic structures, such as giant loops or transequatorial loops (Delannée and Aulanier, 1999), giant filaments or filament channels (Wang, 2002).

The ratio between thermal and magnetic pressure (β) is very small in the low solar corona, $\beta \ll 1$. Therefore, the magnetic energy dominates all other forms of energy in the source regions of solar eruptions (see the review of Forbes, 2000, and the references therein). Current-free (potential) magnetic fields correspond to the minimum magnetic energy for a given distribution of magnetic flux through the dense photosphere. Since the photospheric flux distribution does not significantly change during the time-scales of eruptions, and since the powering of eruptions requires the magnetic energy to decrease, the coronal magnetic field must therefore be highly non-potential prior to the eruption onset, i.e., it must contain strong electric current densities. Due to the slow evolution of the photospheric magnetic field (as compared to typical coronal velocities), currents which are injected into the corona must accumulate slowly, such that the coronal field evolves quasi-statically, as a sequence of force-free equilibria. The triggering of CMEs therefore requires the coronal field to reach some threshold above which the balance between magnetic pressure (which points upward) and magnetic tension (which points downward) is broken. When the system suddenly enters a regime in which the magnetic

* Corresponding author.
E-mail addresses: brigitte.schmieder@obspm.fr (B. Schmieder), guillaume.aulanier@obspm.fr (G. Aulanier).

0273-1177/$36.00
doi:10.1016/j.asr.2011.10.023

pressure dominates, it can erupt in a catastrophic way, leading to a CME. When the CME is initiated and propagating, reconnection is still needed to allow the CME to continue its expansion (Lin and Forbes, 2000).The resulting ideal expansion of the magnetic field, as well as the resistivity driven magnetic reconnection in the current layer that forms in the wake of the expanding system, both contribute to decrease the magnetic energy.

The storage of energy should be detected by the presence of currents in the corona. The currents are aligned along the magnetic field lines as it is observed before eruption. Three different manifestations of the presence of aligned currents are: (i) twisted prominences, (ii) sigmoid-shaped X ray brightenings in the corona, and (iii) emergence of new flux with lane-shaped currents observed in photospheric magnetograms. These observations are well reproduced in many models of CMEs (see the review of CME models in the introduction of Aulanier et al., 2010). Aulanier et al. (2010) discussed the physical mechanisms used to produce CMEs in each model. We proposed in this paper to revisit different sets of observations of eruptions and CMEs with the objective of determining the observational signatures allowing us to answer the different questions: how the currents are increasing in the corona? what kind of instability leads to the eruption? what "storage and release" model is valid to explain the specific observations? We show that the observed structures reach a catastrophic phase, the eruption, by increasing currents or decreasing the restraining forces as suggests the theory. For this purpose, we explore different observations of eruptions, reviewing the respective role of emerging flux, twisting and shearing of the field lines, and reduced background magnetic field, triggering the eruptions. We conclude that the region should have stored enough energy and helicity in order to reach a distance close to some threshold before eruption. Many different physical process occur simultaneously or sequentially like emerging twisted flux tube and decrease of the magnetic field of the overlying arcades. In the last section we discuss the simulation of Aulanier et al. (2010), which allows one to experiment with effects of different parameters and to detect thresholds of loss of equilibrium. Simulations show that one of these processes in itself is generally not efficient to trigger an eruption/CME. The magnetic configurations should first be close to a threshold of equilibrium.

Aulanier et al. (2010) used the simulation as a tool like a new instrument to experiment with the efficiency of what observations suggest as being the important trigger. They conclude that of all the ingredients that may trigger most eruptions, the torus instability (loss of equilibrium of a flux tube) is finally the efficient trigger mechanism in their simulation.

2. Observations and trigger mechanisms

The different CME models show that triggering of CMEs requires the increase of the coronal field to some threshold above which the balance between the magnetic pressure (which points upward) and the magnetic tension (which points downward) is broken and/or the reduction of the tension. Aulanier et al. (2010) in their introduction classified the different existing models of CMEs into:

– Circuit and MHD non-equilibrium models.
– MHD models based on current increase.
– MHD models based on tension reduction.

We will review different papers describing the solar sources of CMEs in order to identify the trigger of the eruption, and discuss possible models.

2.1. Filament eruption

Vršnak et al. (2007) shows that filaments erupt and lead to CMEs when their visually estimated twist is higher than a certain number of turns and when the filament reaches some threshold.

Filippov and Den (2001) studied statistically the height curves of prominences and show that all the prominences reaching a critical altitude were erupting and forming a CME.

During the last solar minimum, between solar cycle 23 and 24, STEREO detected a few erupting filaments. STEREO allows to reconstruct filaments in 3D and determine their velocity (Gosain et al., 2009; Artzner et al., 2010; Bemporad, 2011 for a review). Recent observations of a large eruptive filament have been obtained in September 26, 2009 (Fig. 1, and see also Gosain et al., 2012). A height-time curve of the filament eruption and CME observed by STEREO A and B was reconstructed by a de-projected method (Fig. 2). The curve was confirmed by a tomographic method using "three eyes" after including 304 A TESIS data on board of CORONAS. The height curves show the slow rise of the prominence with no acceleration in the pre-eruptive phase (20 h), then an exponential trajectory of the prominence top in the main phase with a short time period of an acceleration (4 h).

This exponential rise could be a signature of a linearized MHD instability. This instability has been shown to be related to a loss of equilibrium (Démoulin and Aulanier, 2010), which puts it in the same context as past physical models for non equilibria (Forbes and Isenberg, 1991; Isenberg et al., 1993; Forbes et al., 1994; Forbes and Priest, 1995; Lin et al., 1998; Lin et al., 2002; Lin et al., 1995; Isenberg and Forbes, 2007). For flux instability, we consider the torus instability, well studied by different authors (Kliem and Török, 2006; Török and Kliem, 2007; Fan and Gibson, 2007; Schrijver et al., 2008). Aulanier et al. (2010) discussed this instability in their model forming a flux rope (filament) that they called a torus, as in Titov and Démoulin (1999). In the latter, half of the torus is emerged above the solar surface, half is below the photosphere (image current). Without line tying, the half torus can eventually freely expand. The curvature of the torus or "hoop"

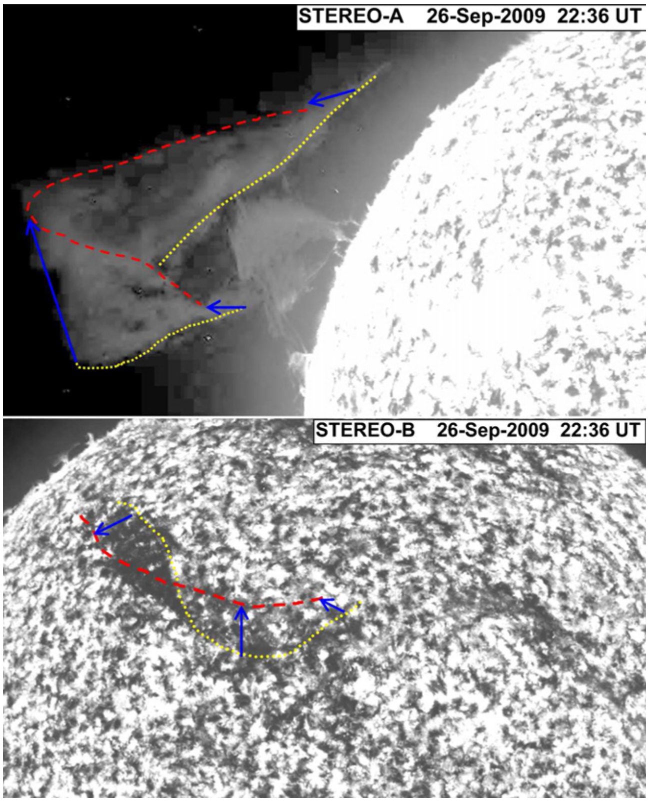

Fig. 1. The STEREO-A and B images of the eruptive filament are shown in top and bottom panels respectively. The filament sheet is shown by dashed (red) and dotted (blue) lines. The sheet appears to be twisted by about 180° along the marked length. The arrows indicate the orientation of the filament sheet. (For interpretation of the references to colour in this figure legend, the reader is referred to the web version of this article.)

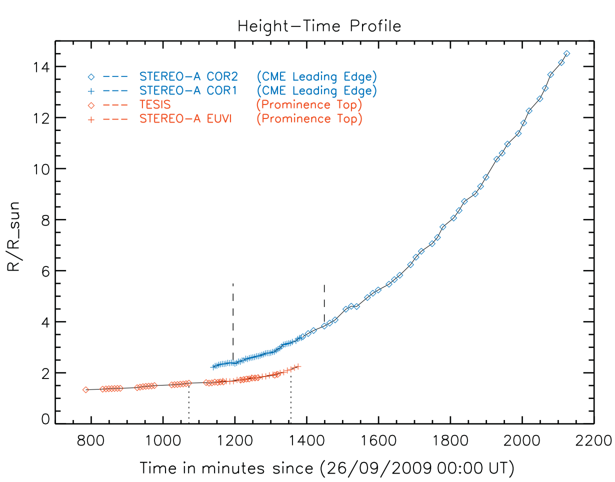

Fig. 2. The lower curve shows the height-time profile of the prominence top, derived from TESIS (diamonds) and STEREO-A (pluses) observations. The upper curve shows the height-time profile of the CME leading edge observed with STEREO-A COR1 (diamonds) and COR2 (pluses). These plane-of-sky height-time curves have been de-projected for the propagation angles. The acceleration phases are between the vertical dashed lines and these curve parts are fitted with an exponential function (Gosain et al., 2012).

force is radially directed. If the external magnetic field is decreasing faster than the hoop force, a torus instability occurs and the torus (flux rope or filament in the observations) erupts. Gosain et al. (2012) suggest that the torus instability may explain the destabilization of the STEREO filament on September 26 2007. The restraining force should be weak because the magnetic environment of the prominence is very low: the arcades over the filament are anchored in network of 3G.

2.2. Emerging flux and shearing

From an observational point of view, we may distinguish which phenomena is important to drive the eruption: emerging magnetic flux or shear motions in the photosphere? An interesting case, carefully analyzed by Chandra et al. (2010, 2011) may help to understand what are the acting forces and the mechanisms leading to the eruptions. The active region NOAA 10501, located in the North Hemisphere was one of the most complex and eruptive regions during the decay phase of Solar Cycle 23. This AR was the successor of the very flare productive active region NOAA 10484, during the Halloween period, in the previous rotation. AR 10501 produced 12 M-class flares, some of them accompanied by CMEs, from 18 to 20 November 2003. In particular, it produced the most geoeffective event of the Solar Cycle 23 (Dst = −457 nT) (Schmieder et al., 2011). It has been associated with a magnetic cloud of positive helicity and to the AR 10501 of global negative helicity. The peculiarity of this AR was that it contained areas of different magnetic helicity signs, as was discussed by Chandra et al. (2010). This is due to the emergence of a new bipole of opposite magnetic helicity sign (positive helicity) of the active region itself.

Chandra et al. (2010) show that in the two days preceding the flares, more than -4×10^{26} Wb^2 (-4×10^{42} Mx^2) of negative helicity were injected in the whole active region. However in the region P4–N4, which is magnetically connected, a total positive helicity of 30×10^{24} Wb^2 has been injected during the same time (Fig. 3). If the injection lasted for 6 days, as it looks to be, an accumulation helicity of the order of 10^{26} Wb^2 would have been injected, enough magnetic helicity to generate a CME and a magnetic cloud (DeVore, 2000; Lynch et al., 2005).

However, was the emergence of this twisted new flux tube responsible for all the flares occurring in this active region? Also, how did the transport of magnetic helicity and flux proceed? On 18 November 2003, Chandra et al. (2010) conclude that the main trigger mechanism is more complex. It is a combination of the emergence of the bipole and the consequent shear of the magnetic polarities between the new flux and the preexisting flux (Fig. 3). In the area of the emerging flux a sigmoid was observed and so were three successive flares. The long filament surrounding the active region had one end in the emerging flux area. This part of the filament located along an inverse magnetic field line in a very sheared region was destabilized several times and erupted while “J-shaped” ribbons were observed as the signature of reconnection. The last two flares are

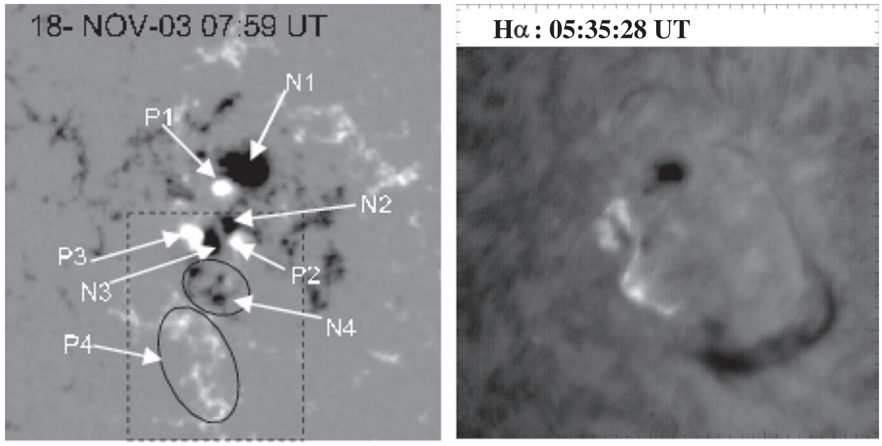

Fig. 3. *Left panel*. Longitudinal magnetic field map of AR 10501 showing the multiple bipoles and their evolution versus time before the eruption. P3N3 is the emerging bipole. N3 rotates around P3 and breaks in many pieces pushing N4 towards the East. These motions induce a large shear along the magnetic inversion line where lies the erupting filament between N4, P4 (represented by the two ovales in the top panel). Positive/negative polarities are represented respectively in white/black. The size of the top image is 370″ × 370″, *right panel* Hα image on 18 November 2003 with a sigmoid (adapted from Chandra et al., 2010).

related to two CMEs of which the second is a halo CME. This large halo CME at 08:50 UT seems to be responsible for the geomagnetic effective magnetic cloud of November 20.

The solar magnetic activity relating to the emerging flux continues during the next few days. On 20 November 2003, Chandra et al. (2011) notice that the negative polarity of the emerging flux (N3 on the 18 November image shown in Fig. 3) is becoming fragmented. In particular, the negative polarity separates into a few small polarities which rotate in a clockwise direction around the positive polarity with large dispersion of the main spots and the network at the periphery. The flare initiation is forced by the continuous motion of the emerging bipole which brings up new helicity.

After having identified the triggering mechanism (emerging flux as the upward force), we can answer the question: how will the ejecta escape? how will the tension force eventually remain lower than the upward force?

MHD models based on removing the tension by magnetic reconnection propose two possibilities. The first possibility is the formation of a vertical current sheet below the emerging flux rope and progressively reconnection occurs below the tube. This model is called “tether-cutting” (Moore et al., 2001). The second possibility is to remove the overlying arcades by coronal reconnection (Antiochos et al., 1999).

On 20 November 2003, two homologous flares leading to two CMEs took place in the active region AR 10501, which has a quadrupolar magnetic configuration. Do the field lines reconnect below the rising flux tube (tether cutting model) or above (break-out model)? The flares exhibit two series of ribbons in Hα the main and secondary ribbons (Fig. 4). The evolution of the ribbons suggests that the first eruption is triggered by “tether cutting” with subsequent quadrupolar reconnection as in the “break-out model”, whereas the second one is consistent with the break-out model directly. The magnetic configuration of the active region is definitively very complex. The active region has all the ingredients (emerging magnetic flux, shear, twist) to get large eruptions but nevertheless it is difficult to write the complete chain of each event.

2.3. Decrease of photospheric magnetic strength

Tether-cutting and break-out models reduce the tension force through magnetic reconnection, however MHD models propose two other possibilities to decrease the tension. They are based on the dispersal of flux in the photosphere. A very popular way to decrease the flux is by flux cancelation via convergence along the magnetic field inversion lines. Many observations and models proposed this possibility for filament eruptions (van Ballegooijen and Martens, 1989; Lin et al., 2002; Schmieder et al., 2006). Another relies on a homogenous magnetic field decrease all over the photosphere or in the strong field regions of an active region (Amari et al., 2000; Amari et al., 2010). In this case the diminution of flux leads to a decrease of the magnetic energy of the open field to a value below that of the current-carrying field (Amari et al., 2000).

The observations of a disappearing filament observed in September 2006 was interpreted by such a model (Schmieder et al., 2008). The main conclusions were the following: the filament globally rises during 24 h with material flowing in both directions and emptying the filament. The flux tube becomes longer with fewer footpoints. This would imply that the field lines no longer have dips but have become loop-like. The material along the field lines has a counter-streaming activity. The filament loses material: mass loss $\sim 10^{15}$ g. The consequent CME occurs with a very slow velocity (100 km/s) according to our interpretation of the LASCO observations. This slow CME is mixed with a

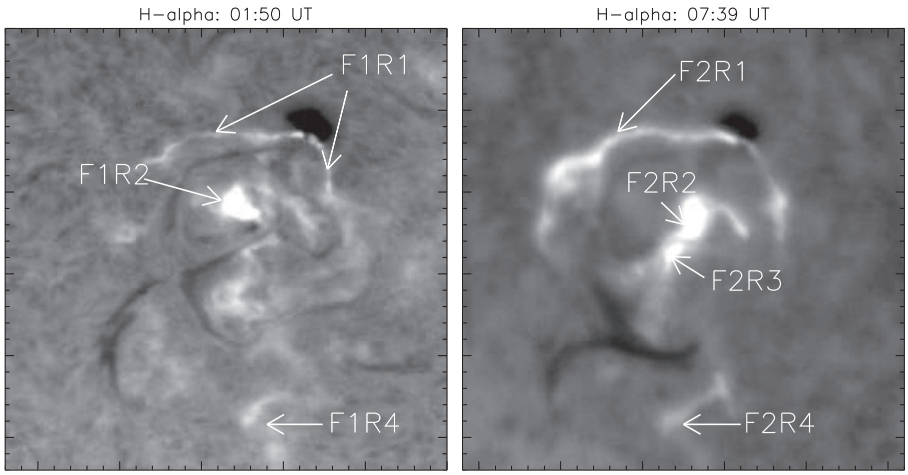

Fig. 4. Flare ribbons on 20 November 2003 observed in ARIES (India).

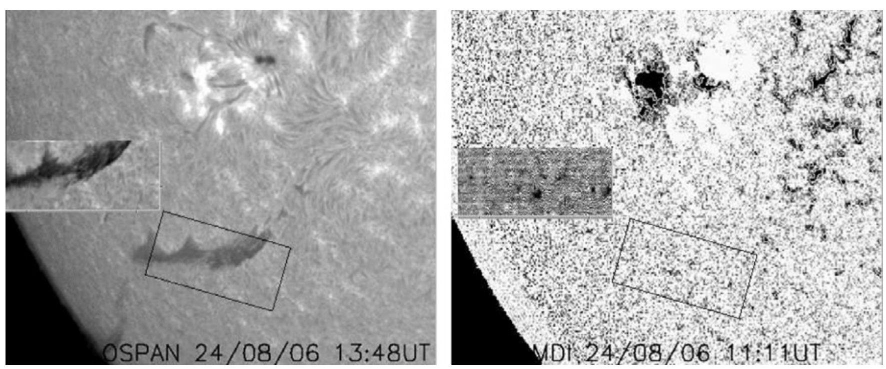

Fig. 5. Co-alignment of THEMIS/MTR observations, OSPAN (left) and MDI (right) (±80 G) for August 24, 2006. The box represents the field-of-view of THEMIS. Over the OSPAN and MDI images we have put a THEMIS image at the same scale on the Hα and magnetic maps.

faster one generated by a flare occurring 10 h later in the active region belonging to the same magnetic system (Fig. 5). Such slow CMEs have previously been detected after filament eruption (Schmieder et al., 2000). We are in a magnetic configuration where there is not a priori magnetic reconnection in the photosphere or in the corona because we do not detect any brightening in Hα and in TRACE 195 Å. No new emerging polarities or cancelling polarities in the filament channel even with the high polarimetry sensitivity of THEMIS were detected (Fig. 5). We measured a relatively large decrease of the photospheric magnetic field strength of the network (from 400 G down to 100 G) which is directly related to filament support. The network has no more strong polarities. This decrease of strength could act as a flux disappearance or loss of confinement and be the reason for the slow filament destabilization and its eruption. The decreasing magnetic field strength is equivalent to tether cutting mechanism in the sense that both diminish the amount of restraining flux above the flux rope.

Simulations of prominence eruption confirm the importance of the photospheric boundary conditions. Amari et al. (1999) modeled a prominence by producing a configuration consisting of a twisted magnetic flux embedded in an overlaying, almost potential, arcade such that high electric currents are confined in the tube. This tube is formed by gradual photospheric diffusion processes. When this process lasts for long enough time, Amari et al. (2000) showed that the magnetic configuration cannot stay in equilibrium so that it leads to a CME. Photospheric diffusion should not produce significant Hα emission, therefore this mechanism may be active in this event. The decrease of the total strength in the field-of-view of THEMIS can be explained by the dispersion of the magnetic field during this time period.

2.4. Emerging flux and filament eruption

Feynman and Martin (1995) studied the association between emerging flux and filament eruptions. They found that in 17 out of 22 cases where newly emerging flux in the vicinity of filaments could be observed, the filament erupted, whereas in the remaining five cases it did not. The new flux typically started to emerge a few days before the eruption, indicating a slow evolution towards an unstable state before the eruption. In 26 out of 31 cases where no emerging flux in the vicinity of the filament was detectable, the filament did not erupt within the period of observation. The authors concluded that filament eruptions are associated with newly emerging flux, but that the latter is not a necessary condition for eruption. In a more recent study, Jing et al. (2004) found that 54 out of 80 filament eruptions were associated with flux emergence. These results indicate that in about 60–70 cases, the vicinity of a filament leads to its eruption. But how can the new flux drive the filament towards eruption? Magnetic reconnection seems to be the key. It was suggested that the emerging flux reconnects with the field overlying the filament and hence destabilizes it (Feynman and Martin, 1995) or decreases its tension to a degree that the core flux cannot longer be stabilized and erupts (Wang and Sheeley, 1999). However, as pointed out in Feynman and Martin (1995) and demonstrated in 2.5D numerical simulations (Chen and Shibata, 2000), the magnetic orientation of the emerging flux with respect to the preexisting coronal field must be favorable for reconnection to occur. However, detailed analytical analyzes in the parameter space of flux models perturbed by neighboring bipoles have revealed that simple arguments based only on the orientation of the bipoles do not provide a complete picture for the occurrence of eruptions (Lin et al., 2001). In the following, we present a recent observation of signatures of such reconnection.

Fig. 6 shows a recent example of flux emergence close to a filament channel observed by Hinode/XRT on 2007 April 24. The bright X-ray loops indicate that reconnection between the emerging flux and the magnetic field overlying the filament took place. Two main bright systems of low loops are visible, one to the left of the filament channel and one arching above the filament, outlining the edge of the filament cavity. We also observed a brightening propagating along this arch in the early phase of the evolution.

The filament is not destabilized by the reconnection and does not erupt in this case. In order to better understand the interaction of the emerging flux with the pre-existing coronal field, and in particular to understand why the filament did not erupt, we aimed to reproduce this event in a numerical simulation (Török et al., 2009). Here we just give a brief description. As initial condition for the simulation they use the analytical model of a bipolar active region by Titov and Démoulin (1999).

EMF and reconnection model is presented in Fig. 7. The model consists of a force-free, line-tied and twisted coronal flux rope embedded in a potential field arcade. Numerical simulations of (Török et al., 2004; Török and Kliem, 2007) have demonstrated that the filament flux rope can be subject to the helical kink instability and the torus instability (Kliem and Török, 2006). The morphological and kinematic evolution of an erupting filament could be successfully reproduced in another simulation (Török and Kliem, 2005). For our purpose, we choose the parameters of the model such that the flux rope is initially stable with respect to both instabilities. We then mimic the emergence of new magnetic flux by successively changing the boundary conditions at the bottom plane of the numerical domain (the photosphere) such that the slow and rigid emergence of another, smaller, flux rope in the vicinity of the pre-existing rope is modelled. We use a technique often referred to as kinematic flux emergence and described in detail in Lin et al. (2001) and in Fan and Gibson (2003). We note that this technique is not supposed to simulate the complex dynamics of realistic flux emergence. Rather it intends to mimic the effect of emerging flux on the dynamics of the coronal field, which is sufficient for our purpose. As the new flux rope slowly emerges, a magnetic null point is formed slightly above it and the rope starts to reconnect with the potential field arcade overlying the TD rope. The amount of flux reconnected depends on the orientation of the magnetic field within the emerging rope with respect to the pre-existing coronal field. We choose the orientation of the ropes field such that it is favourable for reconnection. As the reconnection proceeds, new connectivities are formed (Fig. 5, right panel): field rooted in the positive (white) polarity of the emerging flux rope now close down in neighbouring regions of negative polarity (black) of the model and form low-lying arcades, whereas field lines starting from the negative polarity of the emerging flux rope reconnect with field lines initially overlying the flux rope. The latter exhibits a kinked shape, just as the bright X-ray loop overlying the filament. Although our simulation does not treat the thermodynamics, it is legitimate to qualitatively compare our simulation with the XRT observations, since newly reconnected field lines are expected to be heated and to brighten in X-ray

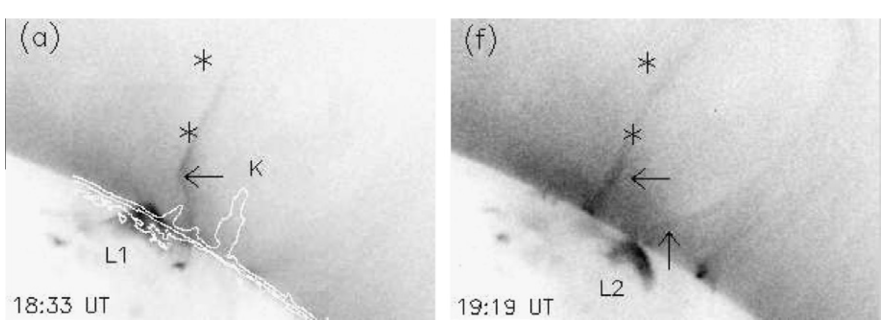

Fig. 6. Coronal cavity observed with Hinode/XRT (reverse colors) surrounding an Hα filament (white contours on the left image). The bright loops L1 and L2 are interpreted as magnetic reconnection due to emerging flux close to filament arcades. K indicate a “kink” in arcade field lines (from Török et al., 2009).

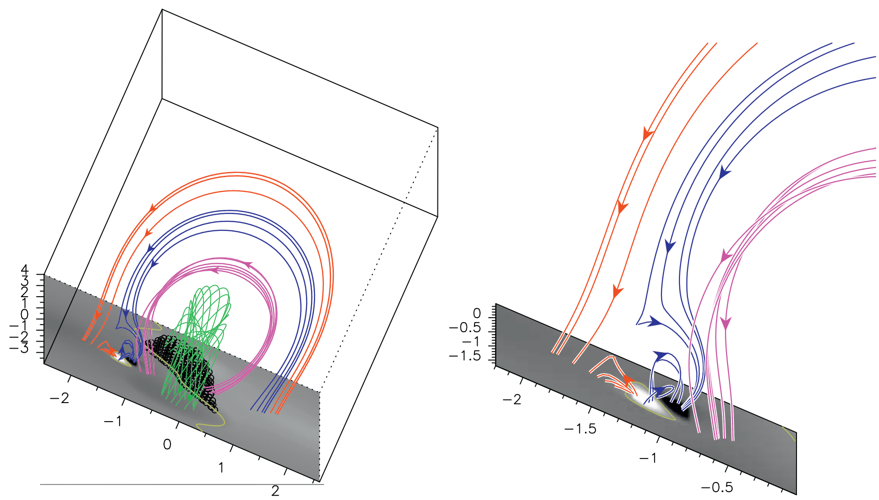

Fig. 7. Modelling of emerging flux close to filament arcades and evidence of low loops from Török et al. (2009).

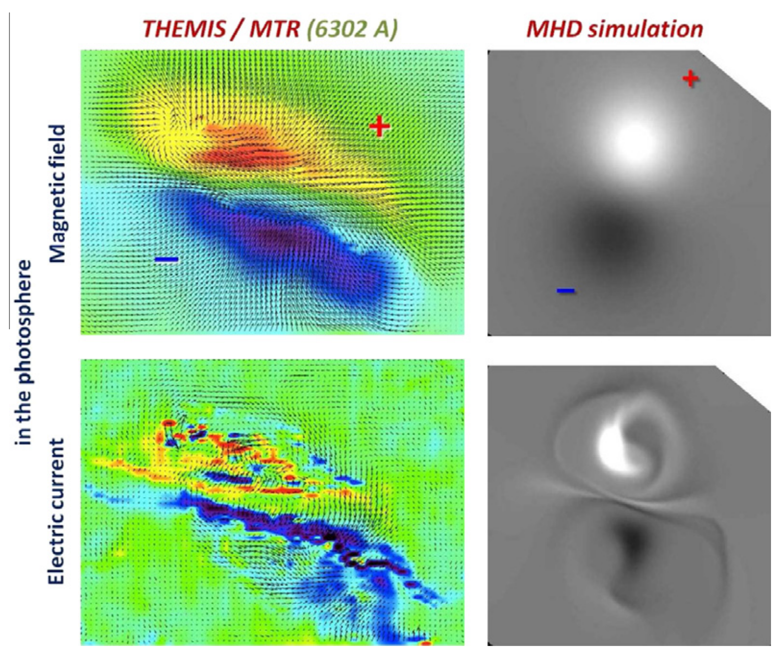

Fig. 8. *Left panels*. Magnetic field observed by THEMIS in the Fe I line 6302A, the arrows represent the transverse field, lane-shape currents in the sunspot compared with *right panels* MHD modelling from Aulanier et al. (2010).

images. The shapes of the newly reconnected field lines are qualitatively similar to the shape of the bright X-ray features, indicating that the simulation reproduces the magnetic interaction between emerging and pre-existing flux in this event reasonably well. As in the real the filament, the initial flux rope does not erupt in our simulation, in spite of a strong neighboring and favorably oriented EMF.

3. Discussion

In their simulation, Aulanier et al. (2010) identified different mechanisms, which have been proposed to lead to eruptions:

(1) dispersing or decreasing magnetic tension,
(2) reconnecting magnetic field below the flux rope,
(3) generating slow and possibly emergence-induced shear-flows.

All the signatures of the presence of currents aligned along the magnetic field are observed in their simulations (currents in the photosphere, sigmoid ribbon in the corona, twisted flux tube) (Figs. 8 and 9). After analyzing their results, they conclude that, in fact, the eruption was due to a torus instability and that the three effects listed above merely drove a slow inflation of the flux tube until its axis reached the threshold of the torus instability.

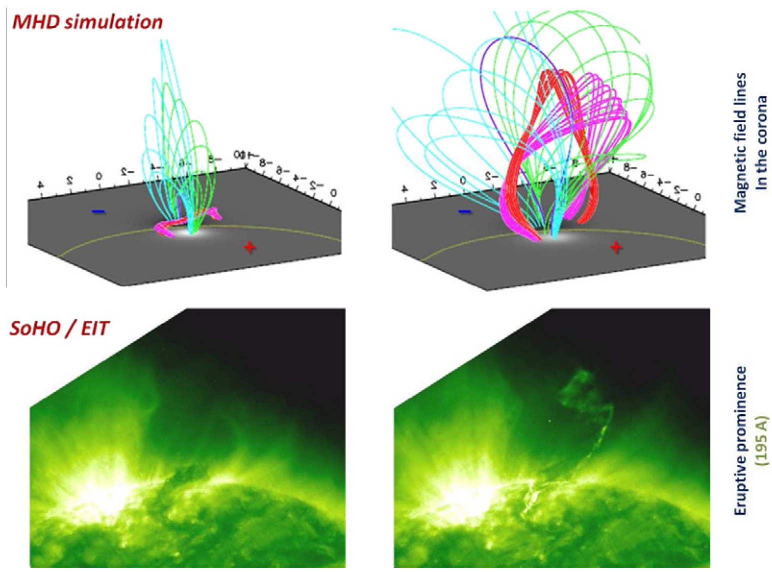

Fig. 9. *Bottom panels*. EIT observations of a filament on the disk and in eruption compared with *top panels* MHD modelling from Aulanier et al. (2010) (the filament are the low pink/red lines). (For interpretation of the references to colour in this figure legend, the reader is referred to the web version of this article.)

We have reviewed different observations where one or more CME drivers have been detected. In particular, observations show that the emerging flux in the vicinity of filaments does not necessarily lead to an eruption. The question arises under which circumstances flux emergence can trigger filament eruptions and CMEs. We think the main factor which decides on the occurrence of an eruption triggered by flux emergence in the vicinity of filaments is how far the pre-eruptive coronal configuration is from an unstable state at the time when the reconnection between the emerging flux and the arcade field above the core flux carrying the filament sets in. The reconnection must sufficiently weaken the tension of the overlying field for the core flux to erupt. How effective the reconnection is in this respect will depend on many factors, as for example the field orientation and the spatial distance of the emerging from the core flux. In cases where the core flux is already close to instability, a small amount of new flux emergence might be sufficient to trigger its eruption, whereas in other cases even a large amount of emerging flux might not be able to drive the system towards an unstable state. It seems that the event (24 April 2007) described above belongs to the latter category. We note that in cases where the new flux emerges just below the filament, it might reconnect directly with the core flux. This could increase the twist of the core flux such that it erupts even if the overlying field is not weakened significantly. Similar conclusions have been drawn in earlier observational, analytical and numerical studies on the relation between emerging flux and solar eruptions.

Acknowledgments

The authors thank CEFIPRA Project 3704-1 for its support of this study on “Transient events in Sun Earth System” during our bilateral collaboration. BS thanks ISSI in Bern where much of this work was carried out analyzed and discussed in the two workshops respectively chaired by Consuelo Cid concerning CMEs and by Klaus Dalsgaard related to the emergence of magnetic flux. BS, GA thank the European network “SOLAIRE” for fruitful discussions with a few network team members. BS thanks Ramesh Chandra for making some figures and the two anonymous referees for their suggestions.

References

Amari, T., Aly, J.J., Mikic, Z., Linker, J. Coronal mass ejection initiation: on the nature of the flux cancellation model. Astrophys. J. Lett. 717, L26–L30, 2010.

Amari, T., Luciani, J.F., Mikic, Z., Linker, J. A twisted flux rope model for coronal mass ejections and two-ribbon flares. Astrophys. J. Lett. 529, L49–L52, 2000.

Amari, T., Luciani, J.F., Mikic, Z., Linker, J. Three-dimensional solutions of magnetohydrodynamic equations for prominence magnetic support: twisted magnetic flux rope. Astrophys. J. Lett. 518, L57–L60, 1999.

Antiochos, S.K., DeVore, C.R., Klimchuk, J.A. A model for solar coronal mass ejections. Astrophys. J. 510, 485–493, 1999.

Artzner, G., Gosain, S., Schmieder, B. A technique for removing background features in SECCHI–EUVI He ii 304 Å filtergrams: application to the filament eruption of 22 May 2008. Solar Phys. 262, 437–447, 2010.

Aulanier, G., Török, T., Démoulin, P., DeLuca, E.E. Formation of torus-unstable flux ropes and electric currents in erupting sigmoids. Astrophys. J. 708, 314–333, 2010.

Bemporad, A. Prominence 3D reconstruction in the STEREO era: a review. J. Atmos. Solar Terrestrial Phys. 73, 1117–1128, 2011.

Chandra, R., Pariat, E., Schmieder, B., Mandrini, C.H., Uddin, W. How can a negative magnetic helicity active region generate a positive helicity magnetic cloud? Solar Phys. 261, 127–148, 2010.

Chandra, R., Schmieder, B., Mandrini, C., Démoulin, P., Pariat, E., Török, T., Uddin, W. Homologous flares and magnetic field topology in active region NOAA 10501 on 20 November 2003. Solar Phys. 269, 83–104, 2011.

Chen, P.F., Shibata, K. An emerging flux trigger mechanism for coronal mass ejections. Astrophys. J. 545, 524–531, 2000.

Delannée, C., Aulanier, G. Cme associated with transequatorial loops and a bald patch flare. Solar Phys. 190, 107–129, 1999.

Démoulin, P., Aulanier, G. Criteria for flux rope eruption: non-equilibrium versus torus instability. Astrophys. J. 718, 1388–1399, 2010.

DeVore, C.R. Magnetic helicity generation by solar differential rotation. Astrophys. J. 539, 944–953, 2000.

Fan, Y., Gibson, S.E. The emergence of a twisted magnetic flux tube into a preexisting coronal arcade. Astrophys. J. Lett. 589, L105–L108, 2003.

Fan, Y., Gibson, S.E. Onset of coronal mass ejections due to loss of confinement of coronal flux ropes. Astrophys. J. 668, 1232–1245, 2007.

Feynman, J., Martin, S.F. The initiation of coronal mass ejections by newly emerging magnetic flux. J. Geophys. Res. 100, 3355–3367, 1995.

Filippov, B.P., Den, O.G. A critical height of quiescent prominences before eruption. J. Geophys. Res. 106, 25177–25184, 2001.

Forbes, T.G., Isenberg, P.A. catastrophe mechanism for coronal mass ejections. Astrophys. J. 373, 294–307, 1991.

Forbes, T.G., Priest, E.R., Isenberg, P.A. the maximum energy release in flux-rope models of eruptive flares. Solar Phys. 150, 245–266, 1994.

Forbes, T.G., Priest, E.R. Photospheric magnetic field evolution and eruptive flares. Astrophys. J. 446, 377–389, 1995.

Forbes, T.G. A review on the genesis of coronal mass ejections. J. Geophys. Res. 105, 23153–23166, 2000.

Gosain, S., Schmieder, B., Venkatakrishnan, P., Chandra, R., Artzner, G. 3D evolution of a filament disappearance event observed by STEREO. Solar Phys. 259, 13–30, 2009.

Gosain, S., Schmieder, B., Artzner, G., Bogachev, S., Török, T. Multi-Spacecraft View of the giant filament eruption on 26–27 September 2009. Astrophys. J., 2012.

Isenberg, P.A., Forbes, T.G., Démoulin, P. Catastrophic evolution of a force-free flux rope: a model for eruptive flares. Astrophys. J. 417, 368–386, 1993.

Isenberg, P.A., Forbes, T.G. A three-dimensional line-tied magnetic field model for solar eruptions. Astrophys. J. 670, 1453–1466, 2007.

Jing, J., Yurchyshyn, V.B., Yang, G., Xu, Y., Wang, H. On the relation between filament eruptions, flares, and coronal mass ejections. Astrophys. J. 614, 1054–1062, 2004.

Kliem, B., Török, T. Torus instability. Phys. Rev. Lett. 96 (25), 255002–255005, 2006.

Lin, J., Forbes, T.G., Priest, E.R., Bungey, T.N. Models for the motions of flare loops and ribbons. Solar Phys. 159, 275–299, 1995.

Lin, J., Forbes, T.G., Isenberg, P.A., Démoulin, P. The effect of curvature on flux-rope models of coronal mass ejections. Astrophys. J. 504, 1006–1019, 1998.

Lin, J., Forbes, T.G. of reconnection on the coronal mass ejection process. J. Geophys. Res. 105, 2375–2392, 2000.

Lin, J., Forbes, T.G., Isenberg, P.A. Prominence eruptions and coronal mass ejections triggered by newly emerging flux. J. Geophys. Res. 106, 25053–25074, 2001.

Lin, J., van Ballegooijen, A.A., Forbes, T.G. Evolution of a semicircular flux rope with two ends anchored in the photosphere. J. Geophys. Res. 107, 1438–1450, 2002.

Lynch, B.J., Gruesbeck, J.R., Zurbuchen, T.H., Antiochos, S.K. Solar cycle-dependent helicity transport by magnetic clouds. J. Geophys. Res. 110, 8107–8117, 2005.

Moore, R.L., Sterling, A.C., Hudson, H.S., Lemen, J.R. Onset of the magnetic explosion in solar flares and coronal mass ejections. Astrophys. J. 552, 833–848, 2001.

Schmieder, B. Magnetic source regions of coronal mass ejections. J. Astrophys. Astron. 27, 139–149, 2006.

Schmieder, B., Aulanier, G., Mein, P., López Ariste, A. Evolving photospheric flux concentrations and filament dynamic changes. Solar Phys. 238, 245–259, 2006.

Schmieder, B., Bommier, V., Kitai, R., Matsumoto, T., Ishii, T.T., Hagino, M., Li, H., Golub, L. Magnetic causes of the eruption of a quiescent filament. Solar Phys. 247, 321–333, 2008.

Schmieder, B., Delannée, C., Yong, D.Y., Vial, J.C., Madjarska, M. Multi-wavelength study of the slow “disparition brusque” of a filament observed with SOHO. Astron. Astrophys. 358, 728–740, 2000.

Schmieder, B., Démoulin, P., Pariat, E., Török, T., Molodij, G., Mandrini, C.H., Dasso, S., Chandra, R., Uddin, W., Kumar, P., Manoharan, P., Venkatakrishnan, P., Srivastava, N. Actors of the main activity in large complex centres during the 23 solar cycle maximum. Adv. Space Res. 47, 2081–2091, 2011.

Schrijver, C.J., Elmore, C., Kliem, B., Török, T., Title, A.M. Observations and modeling of the early acceleration phase of erupting filaments involved in coronal mass ejections. Astrophys. J. 674, 586–595, 2008.

Subramanian, P., Dere, K.P. Source regions of coronal mass ejections. Astrophys. J. 561, 372–395, 2001.

Titov, V.S., Démoulin, P. Basic topology of twisted magnetic configurations in solar flares. Astron. Astrophys. 351, 707–720, 1999.

Török, T., Aulanier, G., Schmieder, B., Reeves, K.K., Golub, L. Fan-Spine Topology Formation Through Two-Step Reconnection Driven by Twisted Flux Emergence. Astrophys. J. 704, 485–495, 2009.

Török, T., Kliem, B. Numerical simulations of fast and slow coronal mass ejections. Astronomische Nachrichten 328, 743–746, 2007.

Török, T., Kliem, B. Confined and ejective eruptions of kink-unstable flux ropes. Astrophys. J. 630, L97–L100, 2005.

Török, T., Kliem, B., Titov, V.S. Ideal kink instability of a magnetic loop equilibrium. Astron. Astrophys. 413, L27–L30, 2004.

van Ballegooijen, A.A., Martens, P.C.H. Formation and eruption of solar prominences. Astrophys. J. 343, 971–984, 1989.

Vršnak, B., Maričić, D., Stanger, A.L., Veronig, A.M., Temmer, M., Roša, D. Acceleration phase of coronal mass ejections: I. Temporal and spatial scales. Solar Phys. 241, 85–98, 2007.

Wang, J.X. Photospheric magnetic fields and the origin of CMEs, in: Hénoux, C. Fang, Vilmer, N. (Eds.), Proceedings of the 2nd French–Chinese meetings. World Publishing Corporation, pp. 145–156, 2002.

Wang, Y.M., Sheeley, J. Filament eruption near emerging bipoles. Astrophys. J. 510, L157–L160, 1999.